Horizon Europe MSCA Project

(Grant Agreement Number 101086219)

Intelligent and Proactive Optimisation for Service-centric Wireless Networks

IPOSEE

D2.1

Performance limits and trade-offs in the interplay of densely deploying APs and modifying the built environment

Authors(s)	Kan Lin, Zhanwei Yu, Di Yuan, Yi Zhao
Author(s) Affiliation	Ranplan Wireless Ltd. UK and Uppsala University, Sweden
Editor(s):	X. Chu, Y. Kritikou, and H. Hu.
Status-Version:	1.0
Project Number:	101086219
Project Title:	Intelligent and Proactive Optimisation for Service-centric Wireless Networks
Project Acronym:	IPOSEE
Work Package Number	2

Table of Contents

List of Figures

List of Tables

Executive Summary

This report presents the first deliverable of work package (WP) two of the IPOSEE project: Joint optimization for service-centric wireless network and propagation environment deployment. The deliverable studies performance and trade-offs in dense deployment of base stations (BSs) with multiple-input-multiple-output (MIMO), and improving the radio propagation environment via intelligent reflective surfaces (IRSs). We present the system models for these deployment scenarios for delivering service to heterogenous traffic demand over the service area. Optimization for configuring MIMO and IRS system parameters is examined, in order to study the capacity performance that can be achieved. Simulations are then performed to numerically characterize and compare the performance of the network densification via BSs and IRSs.

1. Introduction

Mobile communications have evolved to the fifth generation (5G) systems. Today, wireless network infrastructure plays a crucial role in modern society, transforming how people communicate and conduct business. Mobile networks empower businesses through e-commerce, mobile banking, and remote work, enhancing productivity and economic growth. In addition, mobile networks have become vital for all sectors of the society, such as healthcare, education, and emergency response.

Along the technological evolution, two techniques are of particular relevance for improving service quality of mobile networks in 5G and beyond.

- Multiple-Input Multiple-Output (MIMO): MIMO [1] [2] [3] is a key technology to enhance the service coverage and network capacity. This is achieved by using multiple antennas at the transmitter (such as a base station) and the receiver (e.g., a user device), enabling to transmit and receive multiple data streams simultaneously. Deploying MIMO allows to achieve higher data rates and improved coverage, especially in challenging environments with unfavorable conditions for radio signal propagation. Moreover, MIMO enables the same spectrum to be shared by multiple users and hence significantly boosts the efficiency in resource utilization.
- Intelligent Reflective Surface (IRS): The technique uses a surface containing many small and reflecting elements that control how the radio signals are reflected [4] [5] [6]. IRSs are placed in the environment, such as buildings walls, to improve signal propagation by reflecting signals toward intended receivers. Using IRSs enables to overcome obstacles and mitigate interference. In addition, since an IRS does not actively transmit or amplify signals, it is very energy efficient. Deploying IRSs amounts to optimizing the radio propagation environment.

Along with the technological development, new strategies at the network level are necessary as well, to tackle the challenge of rapid growth of data demand that causes congestion. Among them, network densification [7] [8] [9] is an important concept. By network densification, radio base stations (BSs) become more densely deployed, particularly at traffic hotspots. By densification, the distance between the users and their respective serving BSs becomes shorter, enabling stronger signals, higher data rate, and lower latency. Densification also improves spectral efficiency by allowing reuse of spectrum resource in smaller geographic areas, reaching higher network capacity without the need of additional radio resource.

Within the above background, this deliverable studies the performance of MIMO and IRS in the context of network densification in scaling up the network capacity. We provide our system model for multi-cell MIMO and IRS, and characterize the data rate, taking into account inter-cell interference. We then examine the optimization of system parameters in MIMO and IRS, in order to maximize the data rate that can be achieved in the individual BS coverage areas, subject to heterogenous user and demand distributions. The study focuses on the capacity limit, given as the maximum level of data demand that can be served by using MIMO-enabled or IRS-based network

densification. Simulations are performed, to numerically assessing the benefit of densification in capacity improvement.

The remainder of the report is organized as follows. In Section 2, we present the underlying system model as well as the key entities and mathematical notation. Sections 3 and 4 are devoted to performance characterization for multi-antenna BS with MIMO and BS assisted by IRS, respectively. In Section 5, simulation results of MIMO and IRS, in the context of network densification are presented and evaluated. Conclusions are then given in Section 6.

2. Basic System Model

In this section, we provide the components of the basic system model and introduce the mathematical notation. Consider a mobile network of multiple cells with orthogonal frequency-division multiple access (OFDMA), covering a service area with heterogenous data traffic demand.

The set of BSs, or equivalently the set of cells, is denoted by $\mathcal{I} = \{1, \ldots, I\}$, and the set of users in the service area is denoted by $J = \{1, \ldots, J\}$. Each user has a (nominal) value of data demand, denoted by d_j. This demand, in bits, represents the amount of data expected by the user, during the time for which performance is to be characterized. The maximum possible scaling of this demand will be used to represent the network capacity limit. A user is served by the cell having the strongest signal in terms of the path loss. We use $\mathcal{J}_i$ to represent the users served by cell i. The channel gain of BS i and user $j \in \mathcal{J}_i$ is denoted by g_{ij}. The channel gain tells the quality of the radio signal of a BS and each of the users served by the BS, as well as the how the BS signal will affect, in the form of interference, the users served by the other BSs. This basic setup, thus far without including MIMO or IRS, is depicted in Figure 1.

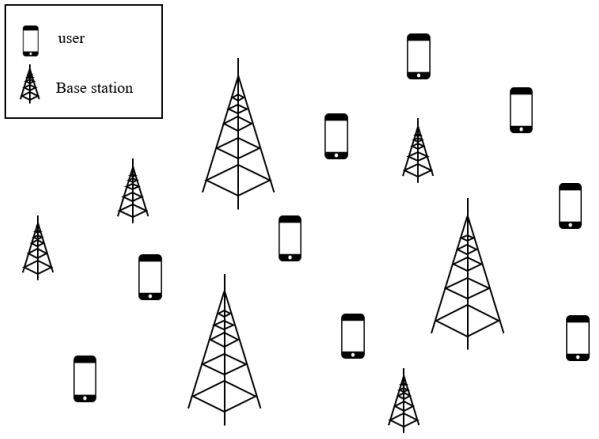

Figure 1. Basic system scenario.

Remark: For simplicity and ease of presentation, the number of cells is treated as a constant in the basic system model. In the context of network densification, the addition of network elements such as micro BSs and IRSs will be examined in Section 5, for which the network density will be scaled up. Moreover, the term user does not necessarily mean one physical network device, as it can be interpreted as a (small) geographic area, and the corresponding demand represents the aggregated value of the area. □

Denote by P_i the transmission power of BS i on a resource block (RB). The signal-to-interference-and-noise ratio (SINR) of and user $j \in \mathcal{J}_i$ is given by the following expression.

$$\mathrm{SINR}_{ij} = \frac{P_i g_{ij}}{\sum_{k \in \mathcal{J} \setminus \{i\}} P_k g_{kj} + n_0}$$

(1)

In Equation (1), entity $\sum_{k \in \mathcal{J} \setminus \{i\}} P_k g_{kj}$ is the total interferences from all other BSs than the serving BS i of user $j \in \mathcal{J}_i$, and n_0 is the thermal noise power. Using the Shannon capacity formula, the corresponding rate, R_{ij}, is given below.

$$R_{ij} = B\log_2\left(1 + \frac{P_i g_{ij}}{\sum_{k \in \mathcal{J} \setminus \{i\}} P_k g_{kj} + n_0}\right)$$

(2)

In Equation (22), B is the bandwidth (in Hertz) of one single RB. Without loss of any generality, it is assumed that the time duration of an RB is one time unit with respect to data rate. Hence, the rate given in Equation (22), in effect, represents also the amount of data delivered to user $j \in \mathcal{J}_i$ on one single RB. Then, the total number of RBs needed in order to meet the demand d_j is obtained as follows.

$$A_{ij} = \frac{d_j}{R_{ij}} = \frac{d_j}{B\log_2\left(1 + \frac{P_i g_{ij}}{\sum_{k \in \mathcal{J} \setminus \{i\}} P_k g_{kj} + n_0}\right)}$$

(3)

Let A denote the total number of RBs with respect to the overall frequency bandwidth and time in question. The data demand of all users served by BS i can be met, that is, the network has sufficient amount of resource for the users of BS i, if $\sum_{j \in \mathcal{J}_i} A_{ij} \leq A$. Thus, for the network as a whole, the resource is sufficient if the following inequality holds.

$$\sum_{j \in \mathcal{J}_i} A_{ij} \leq A, \forall i \in \mathcal{I}$$

(4)

Suppose the above holds as strict inequality for all the BSs, implying that there exists spare resource in the time and frequency domains. We would like to examine the performance limit in the form of capacity that is the overall amount of data demand that can be accommodated with respect to the amount of available resource. Hence, we can use the metric of the maximum possible uniform scaling of the user demand values, such that the resource of at least one BS becomes exhausted. To formally define this metric, note that A_{ij} is a function of demand d_j. Therefore, letting $A_{ij}(d_j)$ denote the function, the overall capacity is defined as follows, where q denotes the demand scaling factor.

$$\max\ q$$

$$\sum_{j \in \mathcal{J}_i} A_{ij}(q d_j) \leq A, \forall i \in \mathcal{I} \tag{5}$$

One can observe that the maximum attainable value of q in (5) can be obtained via bi-section search. That is, given any initial value of q, one examines whether or not the inequality in (5) is met for all the BSs. If the answer is yes, the value of q is doubled, otherwise its value is halved. This is repeated, until the difference of two successive updates is within a defined tolerance interval.

3. Performance Characterization for MIMO

In this section, we build the performance model of MIMO, on top of the basic system model. MIMO is a technique for improving spectrum efficiency, by deploying multiple antenna for signal transmission and reception, as this allows multiple spatial streams to be transmitted concurrently. The concept is illustrated in Figure 2.

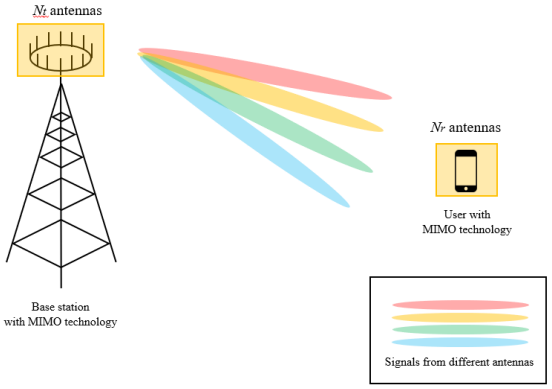

Figure 2. MIMO illustrated.

3.1 MIMO SINR

To proceed, let us assume that a BS as well as any user is equipped with N_t and N_r transmitter and receiver antennas, respectively. For user j served by BS i, the channel condition is given by a channel matrix H_{ij} of size $N_r \times N_t$. This channel matrix represents the wireless channel between the transmitter and receiver antennas. Denote by x_{ij} the transmitted symbol vector of size N_t, and by y_{ij} the receiver signal vector of size N_r. The expression of y_{ij} is as follows, and an illustration is given in Figure 3.

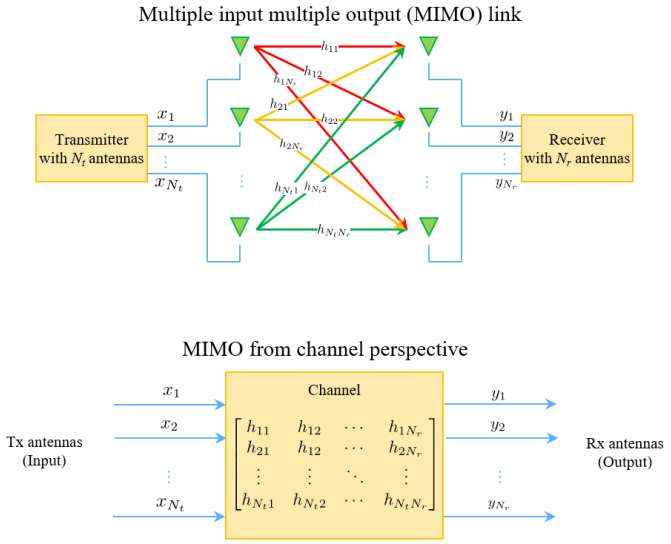

Figure 3. Signal in MIMO.

$$y_{ij} = \sqrt{\frac{E}{N_t}} H_{ij} x_{ij} + \sum_{l \in \mathcal{I}, l/=i} \sum_{k \in \mathcal{J}_\ell} \sqrt{\frac{E}{N_t}} H_{lj} x_{lk} + n_j$$

(6)

The right-hand side of (6 consists of three terms. The first term is the received signal in amplitude on the N_r antennas, governed by the channel matrix between the BS and the user. The second term of two sums represents the total interference. The inner sum is taken over each user k served by BS l, and the outer sum is for all BS l other than BS i. For each user k served by BS l, the symbol transmitted by l to deliver data to user k is x_{lk}, and at user j, this transmission, scaled by the corresponding channel matrix, is the interference received by user j, due to user k of BS l. The last term n_j in (6 is the noise vector, which is assumed to be zero mean circular symmetric complex Gaussian (ZMCSCG). In addition, it is assumed that the transmission power for each transmit antenna is one unit and thus we have the constraint stated in (7).

$$\mathrm{Tr}\left(x_{ij} x_{ij}^T\right) = N_t$$

(7)

With the above, the SINR with respect to power for user j in cell i, that is proportional to the square of its amplitude, is given by the following. It should be noted that the SINR is a function of the signal symbols for transmission for the user in question as well as for the other users.

$$\mathrm{SINR}_{ij}(x) = \frac{\frac{E}{N_t} \left|\left| H_{ij} x_{ij} \right|\right|^2}{\sum_{l \in \mathcal{I} \setminus \{i\}} \sum_{k \in \mathcal{J}_\ell} \frac{E}{N_t} \left|\left| H_{lj} x_{lk} \right|\right|^2 + B n_0}$$

(8)

In terms of capacity as discussed earlier in Section 2, the metric to be examined is the maximum possible scaling factor q, such that the corresponding demand of all users can be accommodated by the network, and this is formulated as follows.

$$\log_2\left(1 + \mathrm{SINR}_{ij}(x)\right) \geq q d_j, j \in \mathcal{J}_i, i \in \mathcal{I}$$

(9)

3.2 Optimizing MIMO Coefficients

Let us consider a generic BS i and user $j \in \mathcal{J}_i$. Maximizing the received signal power amounts to the following optimization task of the MIMO coefficients for this pair of BS and user.

$$\max \ \left|\left|H_{ij}x_{ij}\right|\right|^2$$

$$\mathrm{Tr}\left(x_{ij}x_{ij}^T\right) = N_t$$

(10)

To solve problem (10), one can apply singular value decomposition (SVD) [10] [11] and the water-filling algorithm [12] to determine the optimal values of vector x_{ij}, subject to the power constraint in (10).

SVD is a mathematical technique used to decompose a matrix into three simpler matrices. Specifically, for a MIMO system, where the channel matrix H_{ij} represents the signal paths between the transmitter and receiver, SVD is performed on H_{ij} as follows.

$$H_{ij} = U_{ij}\Lambda_{ij}V_{ij}^T$$

(11)

In (11), the matrices used for decomposition of H_{ij} have the following structure.

- U_{ij} is a unitary matrix and its columns are the left singular vectors corresponding to the receiver side.
- Λ_{ij} is a diagonal matrix containing the singular values (non-negative real numbers) of H_{ij}. These values represent the channel gains of independent subchannels.
- V_{ij} is a unitary matrix and its columns are the right singular vectors corresponding to the transmitter side.

The key benefit of using SVD in MIMO systems is that it transforms the original MIMO channel (a matrix) into multiple independent single-input-single-output subchannels, each associated with one singular value in Λ_{ij}. These subchannels are orthogonal and can be treated separately, simplifying the analysis as well as computation. Essentially, SVD diagonalizes the channel matrix, allowing us to decouple the transmission paths. After applying SVD, one can treat each singular value as the gain of an independent channel, and use the water-filling algorithm to obtain the optimal power allocation for these subchannels.

The water-filling algorithm is a known scheme for optimally allocating power across multiple communication channels or subchannels, especially when these channels are of varying noise levels or channel gains (as in the case with the subchannels generated by SVD). The algorithm works based on the intuition that more power should be allocated to good channels (those with higher gains or singular values), while less power should be given to poor channels (those with lower gains). Mathematically, it can be expressed as the following. Here, P_i is the power allocated to subchannel i, λ is a "water level" that is determined based on the total available transmit power, and σ_i is the square of the singular value in SVD for subchannel i.

$$P_i = \max\left(\lambda - \frac{n_0}{{\sigma_i}^2}, 0\right)$$

(12)

The above formula essentially states that power is only allocated to subchannels where the gain (or inverse noise level) exceeds a certain threshold, and the amount of power increases for subchannels with respect to the gain value.

Determining the optimal water level λ is subject to the total power constraint. The total available power E is allocated across the subchannels, meaning that $\sum_{i=1}^{N} P_i = E$, where N is the number of subchannels. Thus, we have the following constraint.

$$\sum_{i=1}^{N} \max\left(\lambda - \frac{n_0}{{\sigma_i}^2}, 0\right) = E$$

(13)

The steps of computing the water level λ subject to the total power limit are presented below, with an illustration given in Figure 4.

1) Channel sorting: The first step is to sort the subchannels by their inverse channel gain values $\frac{n_0}{{\sigma_i}^2}$ in ascending order. This ensures that power is allocated first to subchannels with better conditions (i.e., those having higher $\frac{n_0}{{\sigma_i}^2}$).
2) Number of active subchannels: Starting with all subchannels being active for power allocation, for each subchannel, one examines whether or not the water level λ exceeds the noise-to-gain ratio $\frac{n_0}{{\sigma_i}^2}$. This corresponds to applying the max-operator as in (12). By this step, which subchannels shall be active become determined.
3) Water level calculation: The water level λ is calculated such that (13) holds. Let N' be the number of active subchannels and $\mathcal{N}'$ the corresponding set, λ is obtained from the equation below.

$$\lambda = \frac{E + \sum_{i \in \mathcal{N}'} \frac{n_0}{{\sigma_i}^2}}{N'}$$

(14)

4) Iterative adjustment: If the calculated water level λ for all subchannels results in allocating more power than E, the number of active subchannels is reduced by one, by excluding the subchannel with the lowest gain. The water level λ is then recalculated considering the remaining active subchannels, and the process is repeated until the sum of allocated power levels equals to the total available.

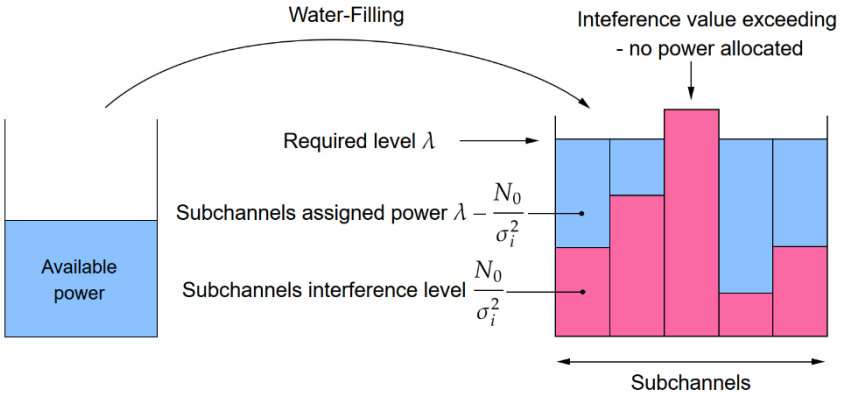

Figure 4. An illustration of the water-filling algorithm.

The procedure of configuring MIMO can be summarized as follows.

1) Apply SVD to the channel matrix H_{ij} to obtain matrices U_{ij}, Λ_{ij}, and V_{ij}^T.
2) Diagonalize the channel into independent subchannels using Λ_{ij}, where each diagonal element (singular value) corresponds to one subchannel's gain.
3) Use the water-filling algorithm to allocate the available transmission power across the subchannels based on their gain values.
4) The optimal signal vector x_{ij}^* is then computed by applying the power allocation to the right singular vectors in V_{ij}.
5) The precoding beamforming scheme uses the right singular matrix V_{ij} for precoding, ensuring that the transmitted signal is optimally shaped for the subchannels.
6) On the receiver side, the left singular matrix U_{ij} is applied for processing, decoupling the received signal into independent subchannel signals.

In algorithmic form, the procedure is presented in Algorithm 1.

Algorithm 1: SVD and Water-filling Algorithm for Optimal Power Allocation

***Input**: Channel matrix H_{ij}, total power E, and noise power n_0*
***Output**: Optimal signal vector x_{ij}^**

Perform SVD on the channel matrix: $H_{ij} = U_{ij}\Lambda_{ij}V_{ij}^T$;
$N \leftarrow$ Number of subchannels;
Extract singular values: $\Lambda_{ij} = [\sigma_1, \sigma_2, \ldots \sigma_N]$;
Initialize power allocation: $P = [0,0,\ldots,0]$;
Sort $\frac{n_0}{\sigma_i^2}$ of all subchannels in ascending order;
$s \leftarrow 0$;
For $i = 1$ **to** N **do**
    $s \leftarrow s + \frac{n_0}{\sigma_i^2}$;
    Compute water level: $\lambda \leftarrow \frac{E+s}{i}$;

If $\lambda \leq \frac{n_0}{\sigma_i^2}$ **then**
  $N' \leftarrow i - 1$;
  break;
End if
End for
For $i = 1$ **to** N' **do**
  Allocate power: $P_i \leftarrow \lambda \frac{n_0}{\sigma_i^2}$;
End for
Compute optimal signal vector: $x_{ij}^* \leftarrow V_{ij}\sqrt{E}$;
Transmitter: Apply re-coding using V_{ij};
Receiver: Apply post-processing using U_{ij};
Return x_{ij}^*;

4. Performance Characterization for IRS

In this section, we examine the use of IRS as part of the radio propagation environment, to achieve more favorable signal reception. Note that adding IRSs to a wireless network infrastructure achieves similar effects of network densification, without deploying additional BSs. In contrast to network densification using regular BSs, IRS passively reflects radio signals and hence consumes much less energy.

4.1 IRS Model

We use the same basic notation as in Section 2. In addition, denote by $\mathcal{L} = \{1, \ldots, L\}$ the set of deployed IRSs in the network. In case one IRS is installed in the service area of each (macro) BS, we have $L = I$. The set of IRSs located in the range of BS i is denoted by $\mathcal{L}_i$. Without loss of generality, we assume that all the IRSs have the same number of reflection elements (denoted by M). Let $\mathcal{M} = \{1, \ldots, M\}$.

With IRS, the signals, from the performance standpoint for a user, consists of three parts that go from the BS to the user directly, from a BS to an IRS, and from the IRS to the user. As in Section 2, the gain of BS i and any of its user j is denoted g_{ij}. For BS i and IRS l, G_{il} is used to denote the $1 \times M$ vector characterizing the channel between the BS and IRS. Furthermore, the $M \times 1$ vector for the channel between IRS l and user j is denoted by H_{lj}. An illustration is given in Figure 5.

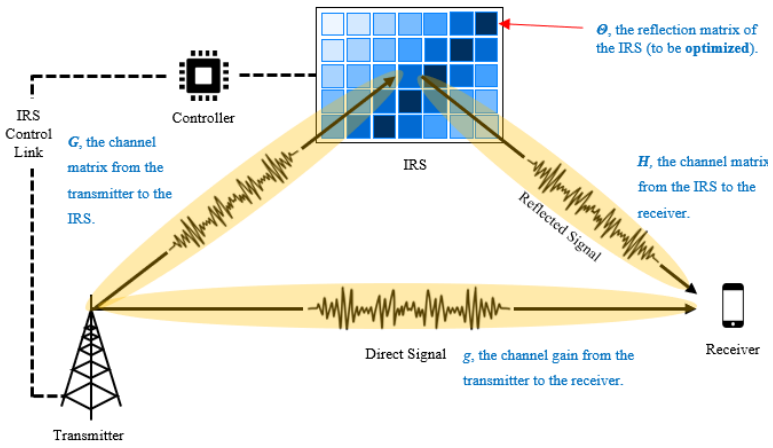

Figure 5. IRS-assisted downlink transmission.

Let $\phi_{lm} = \lambda_{lm} e^{i\theta_{lm}}$ denote the m-th reflection coefficient of the IRS l, where λ_{lm} and θ_{lm} represent its amplitude and phase, respectively. The diagonal reflection matrix of IRS l is then given by

$$\Theta_l = \mathrm{diag}(\phi_{l1}, \phi_{l2}, \ldots, \phi_{lM}) \quad (15)$$

We assume that the amplitude and phase of any reflection element of an IRS can be adjusted independently of each other. Hence, the value domains of the amplitude (after normalization) and phase are as follows.

$$\mathcal{D} = \{\lambda_{lm} e^{i\theta_{lm}} : \lambda_{lm} \in [0,1], \theta_{lm} \in [0,2\pi]\}$$

(16)

4.2 SINR and Rate with IRS

Denote by x_k the signal transmitted by BS k. The overall received signal by user j, including interference, consists of the direct links from the BSs and the indirect links via the IRSs. It is assumed that for a user j of BS i, the IRSs of the BS will contribute to the signal reception as well as reflect interference from the other BSs, whereas the IRSs of the other BSs do not contribute to the signal of interest or interference as they are located much further away from the user. The received signal is then expressed in (17). The first part corresponds to the intended signal including the direct path between a user j of BS i, and those via the IRSs in $\mathcal{L}_\mathrm{i}$. The second part is the interfering signal, while n_j is the additive white noise. Note that g_{kj} and $\sum_{l\in\mathcal{L}_i} G_{kl}\Theta_l H_{lj}$ are the channel gain of the direct interference link and that of the IRS link between another BS k and user j, respectively.

$$y_j = \left(g_{ij} + \sum_{l\in\mathcal{L}_i} G_{il}\Theta_l H_{lj} \right) x_i + \left(\sum_{k\in\mathcal{I}:k/=i} g_{kj} + \sum_{k\in\mathcal{I}:k/=i} \sum_{l\in\mathcal{L}_i} G_{kl}\,\Theta_l H_{lj} \right) x_k + n_j$$

(17)

In the power domain, the interference received by user j is given by the following, where P_k is the transmission power of BS k.

$$\Upsilon_{ij} = \sum_{k\in\mathcal{I}:k/=i} \left| g_{kj} + \sum_{l\in\mathcal{L}_i} G_{kl}\Theta_l H_{lj} \right|^2 P_k$$

(18)

Let $\phi_l = [\phi_{l1}, \phi_{l2}, \ldots, \phi_{lM}]^T$. We have

$$G_{il}\Theta_l H_{lj} = \Lambda_{ijl}\phi_l,$$

(19)

where $\Lambda_{ijl} = G_{il}\mathrm{diag}\{H_{lj}\}$. We therefore have the SINR of user $j \in \mathcal{J}_i$ as follows, with σ^2 being the noise power. Note that the SINR is a function of the IRS reflection configuration ϕ_i that is composed by $\phi_l, l \in \mathcal{L}_i$.

$$\mathrm{SINR}_{ij}(\phi_i) = \frac{\left| g_{ij} + \sum_{l\in\mathcal{L}_i} \Lambda_{ijl}\Phi_l \right|^2 P_i}{\sum_{k\in\mathcal{I},k/=i} \left| g_{kj} + \sum_{l\in\mathcal{L}_i} \Lambda_{kjl}\Phi_l \right|^2 P_k + \sigma^2}$$

(20)

4.3 Optimizing IRS Reflection Coefficients

In terms of network capacity, we seek the maximum possible scaling q of the user demand in the network, such that the scaled demand can be met. This leads to the following optimization problem for BS i.

$$\text{[P1]} \max_{\phi} \; q$$

$$\log_2\left(1+\text{SINR}_{ij}(\phi_i)\right) \geq q\text{d}_j, j \in \mathcal{J}_i \quad \text{(21a)}$$

$$\phi_{lm} \in \mathcal{D}, m \in \mathcal{M}, l \in \mathcal{L}_i \quad \text{(21b)}$$

(21)

It can be observed that the rate inequality above is non-convex. To proceed, we first introduce auxiliary variables γ_j, $j \in \mathcal{J}_i$, to represent the SINR of the users. Then problem P1 can be stated as P2 below.

$$\text{[P2]} \max_{\phi,\gamma} \; q$$

$$\log_2(1+\gamma_j) \geq q d_j, \text{j} \in \mathcal{J}_i \quad \text{(22a)}$$

$$\text{SINR}_{ij}(\phi_i) \geq \gamma_j, j \in \mathcal{J}_i \quad \text{(22b)}$$

(21b)

(22)

With respect to variables γ, (22a) is a convex constraint. However, (22b) is not convex. Consider adding another set of auxiliary variables β_j, $\text{j} \in \mathcal{J}_i$, with constraints below.

$$\sum_{k\in\mathcal{I},k/=i} \left| g_{kj} + \sum_{l\in\mathcal{L}_i} \Lambda_{kjl}\Phi_l \right|^2 P_k + \sigma^2 \leq \beta_\text{j}, \text{j} \in \mathcal{J}_i$$

(23)

Proposition 1. Constraint (23 is convex.

Proof: One can note that

$$\left| g_{kj} + \sum_{l\in\mathcal{L}_i} \Lambda_{kjl}\Phi_l \right|^2 = \left(g_{kj} + \sum_{l\in\mathcal{L}_i} \Lambda_{kjl}\Phi_l \right)\left(g_{kj}^* + \sum_{l\in\mathcal{L}_i} \Phi_l^H \Lambda_{kjl}^H \right)$$

where $(\cdot)^*$ and $(\cdot)^H$ denote conjugate and transpose-conjugate. The above, in turn, equals the following.

$$\sum_{l\in\mathcal{L}_i} \Phi_l^H \Lambda_{kjl}^H \Lambda_{kjl}\Phi_l + 2\mathcal{R}\{g_{kl}^* \sum_{l\in L_i} \Lambda_{kjl}\Phi_l\} + \left|g_{kj}\right|^2$$

Here, $\mathcal{R}$ denotes the real part of a complex number. One can see that the first sum above is a second-order cone, and the second term is affine, and the results follows. □

With auxiliary variables β_j, $j \in \mathcal{J}_i$, the SINR constraint in (22 can be re-written as follows.

$$[\text{P3}] \max_{\phi,\gamma,\beta} q$$

(21b), (23)

$$\left| g_{ij} + \sum_{l \in \mathcal{L}_i} \Lambda_{ijl} \Phi_l \right|^2 P_i + \sigma^2 \geq \beta_j \gamma_j, j \in \mathcal{J}_i \tag{24}$$

It is easy to see that there is a one-to-one mapping of the solutions of problems P2 and P3, and hence we have the following result.

Proposition 2. Problem P1 and P2 are equivalent.

In P3, (21b) are (23) are convex, but the SINR constraint is not. To deal with it, one can apply the transformation of $\beta_j \gamma_j = \frac{1}{4}\left((\beta_j + \gamma_j)^2 - (\beta_j - \gamma_j)^2 \right)$, to obtain the following equivalent constraint.

$$(\beta_j + \gamma_j)^2 - (\beta_j - \gamma_j)^2 - 4P_i \left| g_{ij} + \sum_{l \in \mathcal{L}_i} \Lambda_{ijl} \Phi_l \right|^2 \leq 0, j \in \mathcal{J}_i \tag{25}$$

As the next step, the left-hand side of (25) is treated as a function of β, γ, and ϕ.

$$F_j(\gamma_j, \beta_j, \phi_i) = (\beta_j + \gamma_j)^2 - (\beta_j - \gamma_j)^2 - 4P_i \left| g_{ij} + \sum_{l \in \mathcal{L}_i} \Lambda_{ijl} \Phi_l \right|^2, j \in \mathcal{J}_i \tag{26}$$

It can be observed that function F is in fact the difference of convex (DC) functions, and therefore DC programming techniques [13] [14] can be applied. The first-order Taylor expansion of $(\beta_j - \gamma_j)^2$ at point (b_j, c_j) takes the following expression.

$$(\beta_j - \gamma_j)^2 = 2(b_j - c_j)(\beta_j - \gamma_j) - (b_j - c_j)^2 + \zeta(\beta_j, \gamma_j) \tag{27}$$

In the above, $\zeta(\beta_j, \gamma_j)$ denotes the remainder of the Taylor expansion. Since $(\beta_j - \gamma_j)^2$ is convex, $\zeta(\beta_j, \gamma_j) \geq 0$. By combining (26) and (27), we obtain the inequality below.

$$(\beta_j - \gamma_j)^2 \geq 2(b_j - c_j)(\beta_j - \gamma_j) - (b_j - c_j)^2$$

(28)

For the last part of (26), a similar derivation can be done for given point O_l of $\Phi_l, l \in \mathcal{L}_i$, and ξ_{ij} of g_{ij}, to obtain the inequality below, where $(\cdot)^*$ and $(\cdot)^H$ denote conjugate and transpose-conjugate, and $\mathcal{R}$ denotes the real part of a complex number.

$$\left|\xi_{ij} + \sum_{l \in \mathcal{L}_i} \Lambda_{ijl}\, \Phi_l\right|^2 = \left(\xi_{ij} + \sum_{l \in \mathcal{L}_i} \Lambda_{ijl}\, \Phi_l\right)\left(\xi_{ij}^* + \sum_{l \in \mathcal{L}_i} \Phi_l^H \Lambda_{ijl}^H\right)$$

$$= \left|\sum_{\mathrm{l} \in \mathcal{L}_i} \Lambda_{\mathrm{ijl}}\, \Phi_{\mathrm{l}}\right|^2 + 2\mathrm{R}\left(\xi_{\mathrm{ij}} \sum_{\mathrm{l} \in \mathcal{L}_i} \Phi_{\mathrm{l}}^{\mathrm{H}} \Lambda_{\mathrm{ijl}}^{\mathrm{H}}\right) + \left|\xi_{\mathrm{ij}}\right|^2$$

$$\geq 2\mathrm{R}\left\{\left(\xi_{ij} + \sum_{l \in \mathcal{L}_i} \Lambda_{ijl} \mathrm{O}_l\right)^* \left(\sum_{l \in \mathcal{L}_i} \Lambda_{ijl} \Phi_l\right)\right\} - \left|\sum_{\mathrm{l} \in \mathcal{L}_i} \Lambda_{\mathrm{ijl}}\, \mathrm{O}_{\mathrm{l}}\right|^2 + \left|\xi_{ij}\right|^2$$

(29)

The one can define a new function as follows.

$$\widetilde{F}_j(\gamma_j, \beta_j, \phi_i) = (\beta_j + \gamma_j)^2 - 2(b_j - c_j)(\beta_j - \gamma_j) - (b_j - c_j)^2$$

$$-4P_i\left(2\mathrm{R}\left\{\left(\xi_{ij} + \sum_{l \in \mathcal{L}_i} \Lambda_{ijl} \mathrm{O}_l\right)^* \left(\sum_{l \in \mathcal{L}_i} \Lambda_{ijl} \Phi_l\right)\right\} - \left|\sum_{\mathrm{l} \in \mathcal{L}_i} \Lambda_{\mathrm{ijl}}\, \mathrm{O}_{\mathrm{l}}\right|^2 + \left|\xi_{ij}\right|^2\right), j \in \mathcal{J}_i$$

(30)

By the constructions made, the new function defined by (30) is equal or above the value curve of the original function.

Proposition 3. $F_j(\gamma_j, \beta_j, \phi_j) \leq \widetilde{F}_j(\gamma_j, \beta_j, \phi_j)$.

By the above, the following inequality is used to approximate (25). Note that by Proposition 3, any point satisfying the inequality below is guaranteed to satisfy (25).

$$\widetilde{F}_j(\gamma_j, \beta_j, \phi_j) \leq 0, j \in \mathcal{J}_i$$

(31)

It is important to note that function $\widetilde{F}_j(\gamma_j, \beta_j, \phi_i)$ is a sum of convex functions (including affine functions), thus the approximate constraint (31) is convex. Therefore, we arrive at the following convex optimization problem.

$$[\text{P4}] \max_{\phi,\gamma,\beta} \; q$$

(21b), (23), (31)

5. Simulation Results

5.1 Simulation Setup

For simulation and performance evaluation, we start with a basic setup of seven macro BSs, with 20 users randomly and uniformly located in the service area of each BS. This is illustrated in Figure 6.

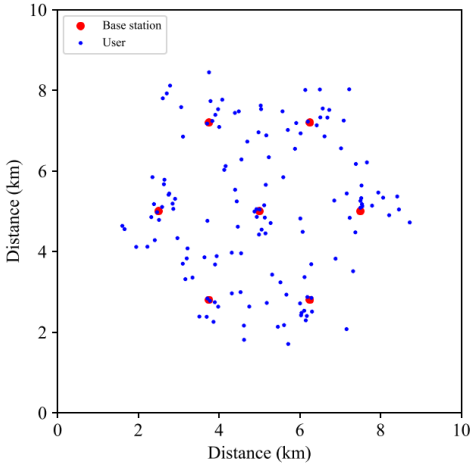

Figure 6. Basic system setup.

The basic setup is used as the reference level of performance in terms of capacity (i.e., maximum uniform scaling of user data demand that can be accommodated). It is then augmented with the following schemes for performance evaluation and comparison.

- Densification: In this scheme, the network is densified by adding ten micro BSs for each macro BS.
- Basic + MIMO: This is the basic setup but with MIMO enabled for multiple antennas; it is assumed a BS uses 16 antennas and the user at the receiver side has 4 antennas.
- Basic + IRS: In this case, the network is densified by adding three IRSs to each BS' area.
- Basic + MIMO + IRS: As indicated by the name, this is the combination of using MIMO and densification with IRS.
- Densification + MIMO: This setup corresponds to adding MIMO to the densified network with macro and micro BSs.
- Densification + IRS: This setup corresponds to adding IRSs to the densified network with macro and micro BSs.
- Densification + MIMO + IRS: As the last scheme, MIMO and IRS are both used in conjunction with the densified network with macro and micro BSs.

It is expected that the more system elements introduced, the higher the capacity. However, it is important to quantify the performance gain enabled by the various schemes since there is a cost-performance trade-off.

The channel between and cell i and user j is given by $g_{ij} = D_{ij}^{-\alpha_{cu}} g_0$, where D_{ij} denotes the distance between the BS of cell i and user j, α_{cu} is the path loss exponent, and g_0 follows a Rayleigh distribution. Similarly, the channel between the BS of cell i and IRS l is given by $G_{il} = D_{il}^{-\alpha_{ci}} G_0$, and the channel from IRS l to user j is given by $H_{lj} = D_{lj}^{-\alpha_{iu}} H_0$. The parameter values used in the simulations are given in Table 1.

Parameter	**Specification**
Number of users per macro BS	20
Macro cell radius	1 km
Carrier frequency	2 GHz
Total bandwidth	20 MHz
Path loss model	COST-231-HATA [15] [16]
Shadowing (Log-normal)	6 dB standard deviation
Fading	Rayleigh flat fading
Power (per resource block) of macro BS	200 mW
Power (per resource block) of micro BS	50 mW
Noise power spectral density	−174 dBm/Hz
Direct path loss exponent α_{cu}	3.5
BS-IRS path loss exponent α_{ci}	2.2 / 4.8
IRS-user path loss exponent α_{iu}	2.2 / 4.8

Table 1. Simulation parameters.

When IRS is present, a comparison of capacity with good and poor IRS propagation is made, in order to gain a comprehensive performance figure. In the former case, the path loss exponents for BS-IRS link and the IRS-user link are set to 2.2. For the latter, an exponent value of 4.8 is used.

In Figure 7, the probability density function (PDF) of the path loss values of the users (with respect to the serving BS) in the basic system scenario is shown. One can observe that the CDF assembles a normal distribution, with a mean path loss of approximately 85 dB. The scenario does not have a bias toward the proportion of cell-center and cell-edge users.

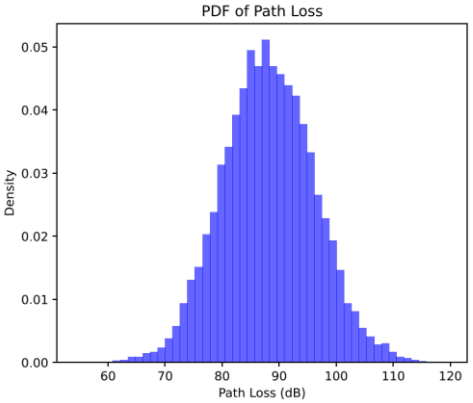

Figure 7. Probability density function of user path loss.

5.2 Performance Result in Capacity

The performance results of network capacity are shown in Figure 8. the maximum possible scaling of user demand is used to represent network capacity.

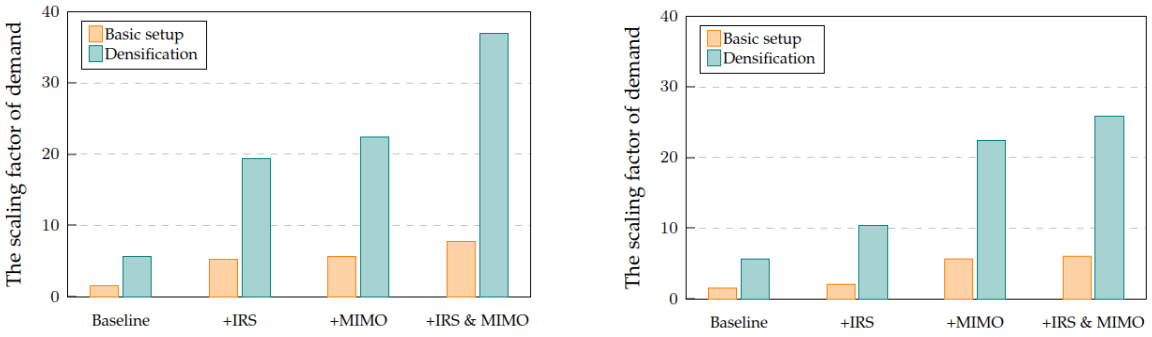

(a) Comparison of capacity with good IRS propagation environemnt.

(b) Comparison of capacity with poor IRS propagation environemnt.

Figure 8. Capacity comparison with two different path loss exponent values for schemes with IRS, where the base demand is 1 Mbps per user and number of reflection elements of an IRS equals 100.

From Figure 8(a), by deploying IRS, the capacity is about four times in comparison to the basic setup. A similar amount of capacity improvement can be obtained by deploying MIMO. A combined use of both boosts the capacity further, which becomes about six times of that of the basic setup. Therefore, both techniques as well as their joint use are effective for improving capacity. From the same figure, one can observe that a basic network densification (without IRS or MIMO) gives a similar effect as deploying IRS or MIMO in increasing capacity. The improvement becomes much more by combining densification with IRS or MIMO - the capacity is increased by a factor of approximately 13. Here, MIMO gives slightly better performance than IRS. Moreover, with a joint use of densification, and IRS as well as MIMO, the additional improvement is very significant; the capacity can be scaled up by a factor of about 25.

From Figure 8(b), the performance of those schemes that include the use of IRS are clearly impacted, if the IRSs have a poor propagation environment. Note that the performance gain due to IRS in the densified network is still clearly noticeable. On the other hand, with MIMO and densification by micro BSs, adding IRSs gives only

moderate performance boost. It is worth pointing out that the performance comparison here assumes 100 reflection elements of each IRS. As will be seen later on, having more elements does help the performance of IRS.

5.3 Performance in Cell Load

The next part of performance study is the resource consumption of the various schemes for given user demand. This metric, referred to as cell load [17], represents the proportion of time-frequency RBs that become occupied in the cell due to delivering the data traffic demand of the cell's users. We focus on the seven macro cells, and examine how MIMO and IRS, as well as densification influence the resource consumption.

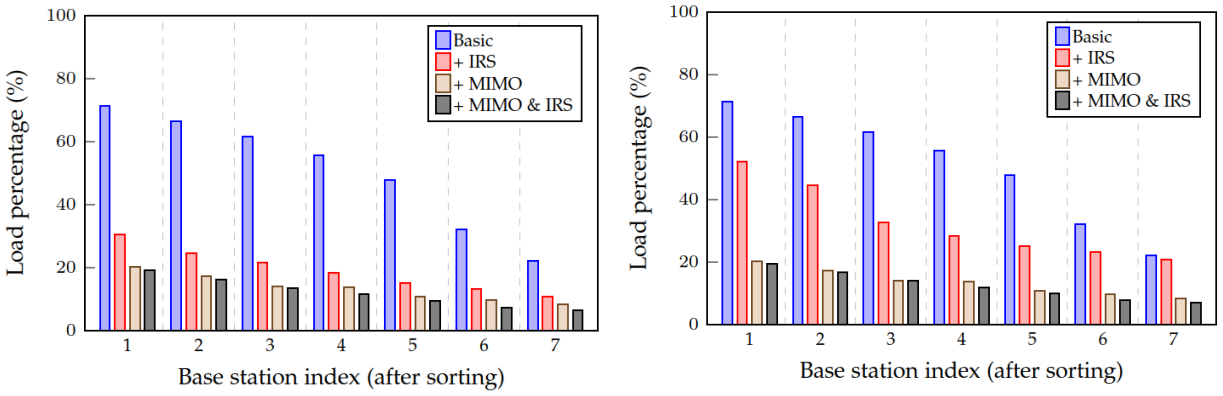

(a) Cell load with good IRS propagation environemnt.

(b) Cell load with poor IRS propagation environemnt.

Figure 9. Cell load of macro BSs without network densification, where data demand is 1 Mbps per user and the number of reflection elements of an IRS equals 100.

The results of the basic setup, and those by using MMO and IRS, without network densification with any micro cell, are shown in Figure 9. The seven macro cells are sorted in descending order of cell load. Without using MIMO or IRS, the cell load is approximately in the range of [0.3, 0.7]. Assuming a favorable IRS propagation environment, by Figure 9(a), adding IRSs reduces the resource consumption by more than 50%, and the effect is largest for the most congested cell. Deploying MIMO gives an even better result – the highest cell load is reduced by almost 60%, and combining MIMO and IRS yields additional gain though the amount is moderate. One can also see that the benefit of joint use is smaller for cells that are congested. For a poor IRS propagation environment, IRS brings, as expected, less benefit, as shown in Figure 9(b), even though the improvement in resource utilization is still noticeable for the most congested cell. It is worth noting that combining MIMO with IRS still gives slight performance gain, even with poor IRS propagation environment.

It is of interested to understand how much MIMO and IRS bring, in comparison to network densification, as well as the effect of them together on cell load. The results are presented Figure 10. One shall pay attention to that the scale of the vertical axis in Figure 10 is different than that of Figure 9.

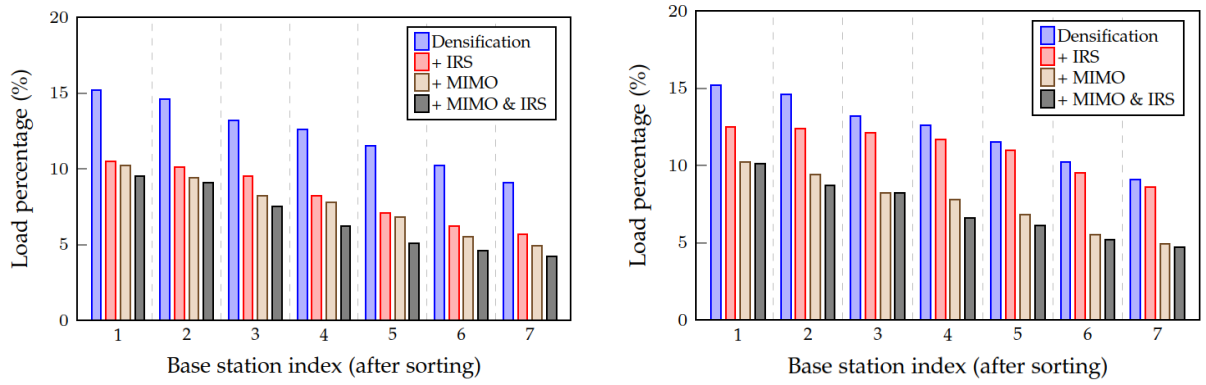

(a) Cell load with good IRS propagation environemnt.

(b) Cell load with poor IRS propagation environemnt.

Figure 10. Cell load of macro BSs with network densification, where data demand is 1 Mbps per user and the number of reflection elements of an IRS equals 100.

The first and immediate observation is that network densification by means of micro cells leads to tremendous reduction of network resource consumption, in comparison to the basic setup. For the most congested cell, the load is reduced from above 0.7 to 0.15; thus the improvement factor is close to five. The reduction is less significant in the other cells but remains very significant. This demonstrates that network densification is very effective. By using MIMO or IRS (assuming a favorable propagation environment for the latter), the improvement becomes even higher, though the relative reduction of resource consumption is less than what can be achieved by these techniques without first applying densification. It is noted again that the gain due to MIMO is somewhat larger than IRS. If the IRS propagation environment is poor, it can still give some improvement though the effect is visible for the cells with high load levels only. After network densification, combining MIMO and IRS is meaningful, only under favorable IRS propagation conditions.

From the above results, it can be concluded that densification via adding micro BSs brings higher performance than modifying the signal propagation with IRS. One can observe that by deploying IRS only, the resource consumption can be cut by more than half as long as the IRS propagation environment is good. With densification, the reduction approaches 80%. However, one shall bear in mind that, in deployment, a BS is more costly than an IRS. Moreover, since IRS targets optimizing signal reflection than active transmission, it also has lower energy consumption. Therefore, there is a trade-off of performance versus cost and energy efficiency. Based on the results, introducing densification to some extent though not aggressively, along with modifying the environment with IRSs, is likely the best choice of addressing the cost-benefit trade-off.

5.4 Performance with Respect to the Number of IRS Elements

As acknowledged earlier, the results presented have been obtained by assuming that each IRS has 100 reflection elements. In reality, it is possible to have a larger number of reflection elements with a comparable deployment cost. Hence it is relevant to understand how scaling up the size of an IRS would benefit the performance, and the results are displayed in Figure 11.

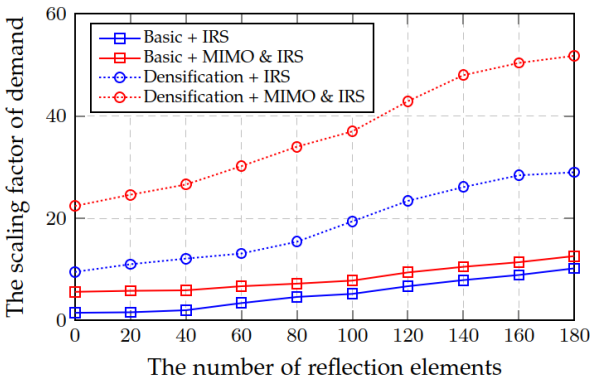

(a) Capacity with good IRS propagation environemnt.

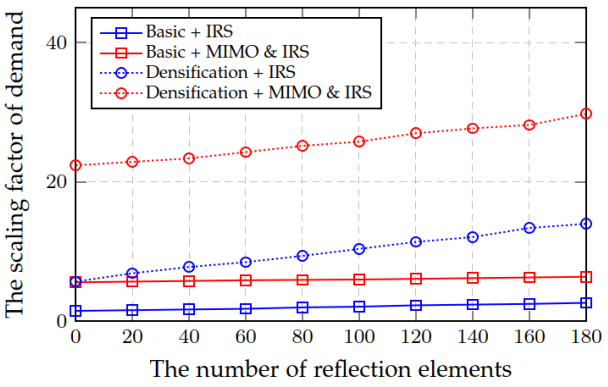

(b) Capacity with poor IRS propagation environemnt.

Figure 11. Network capacity with respect to the number of IRS reflection elements.

From Figure 11, with a favorable IRS propagation environment, the number of reflection elements does have a clear effect on network capacity. For the basic setup as well as for MIMO, having IRS and increasing the number of elements from 100 to 180 almost doubles the capacity. As can be expected, the increase in capacity becomes more significant with respect to the number of elements, when network densification is in place. Note that even if the IRS propagation environment is poor, it still helps under network densification. Thus, network densification with a reasonable cost-benefit trade-off, is a promising approach, and there is a synergy of densification and modifying signal environment with IRSs.

6. Conclusions

In this deliverable, the IPOSEE project has investigated the performance of dense deployment of base station (BSs), in the form of network densification, and its interplay with intelligent reflective surface (IRS) that can improve the radio propagation environment. The deliverable has also studied the effect of multi-antenna systems with multiple-input-multiple-output (MIMO). To have a unified performance characterization, network capacity limit, in terms of the maximum level of user demand that can be accommodated within the time-frequency resource limit, has been used as the main metric for the various schemes and deployment scenarios. In addition, methods for optimizing and MIMO and IRS systems parameters have been studied.

There are a few key finding by the simulation results. First, MIMO, when used alone, clearly can boost network capacity and reduce resource consumption. Since the BSs and user devices are now largely supporting MIMO, what is probably more interesting in the context of IPOSEE project is the effect of modifying the physical radio propagation environment. To this end, network densification offers a dramatic performance improvement, which, however, comes at the price of deployment cost. The use of IRS, by itself, if the IRS propagation environment is favorable, gives a considerable capacity increase, and the joint use of IRS and MIMO, and that with network densification, is highly relevant for gain additional performance benefits. Furthermore, the performance via IRS does improve in the number of reflection elements. Finally, given that deploying IRSs is both easier and less costly then network densification by adding new BSs, a moderate amount of densification, combined with deployment of IRSs, is expected to achieve the optimal performance-cost tradeoff.

References

[1] L. Lu, G. Y. Li, A. L. Swindlehurst, A. Ashikhmin, and R. Zhang, "An Overview of Massive MIMO: Benefits and Challenges," *IEEE Journal of Selected Topics in Signal Processing*, vol. 8, no. 5, pp. 742-758, 2014.

[2] E. G. Larsson, O. Edfors, F. Tufvesson, and T. L. Marzetta, "Massive MIMO for next generation wireless systems," in *IEEE Communications Magazine*, vol. 52, no. 2, pp. 186-195, 2014.

[3] Z. Wang, J. Zhang, H. Du, D. Niyato, S. Cui, B. Ai, K. B. Letaief, and H. V. Poor, "A Tutorial on Extremely Large-Scale MIMO for 6G: Fundamentals, Signal Processing, and Applications," *IEEE Communications Surveys & Tutorials*, vol. 26, no. 3, pp. 1560-1605, 2024.

[4] Q. Wu and R. Zhang, "Towards Smart and Reconfigurable Environment: Intelligent Reflecting Surface Aided Wireless Network," in *IEEE Communications Magazine*, vol. 58, no. 1, pp. 106-112, 2020.

[5] Ö. Özdogan, E. Björnson, and E. G. Larsson, "Intelligent Reflecting Surfaces: Physics, Propagation, and Pathloss Modeling," *IEEE Wireless Communications Letters*, vol. 9, no. 5, pp. 581-585, 2020.

[6] S. Gong, X. Lu, D. T Hoang, D. Niyato, L. Shu, D. I. Kim, Y.-C Liang, "Toward Smart Wireless Communications via Intelligent Reflecting Surfaces: A Contemporary Survey," *IEEE Communications Surveys & Tutorials*, vol. 22, no. 4, pp. 2283-2314, 2020.

[7] N. Bhusha, J. Li, D. Malladi, R. Gilmore, D. Brenner, A. Damnjanovic, R. T. Sukhavasi, C. Patel, and S. Geirhofer, "Network Densification: The Dominant Theme for Wireless Evolution into 5G," *IEEE Communications Magazine*, vol. 52, no. 2, pp. 82-89, 2014.

[8] Y. L. Lee, D. Qin, L. -C. Wang, and G. H. Sim, "6G Massive Radio Access Networks: Key Applications, Requirements and Challenges," *IEEE Open Journal of Vehicular Technology*, vol. 2, pp. 54-66, 2021.

[9] Z. Li, H. Hu, J. Zhang, and J. Zhang, "Enhancing Indoor mmWave Wireless Coverage: Small-Cell Densification or Reconfigurable Intelligent Surfaces Deployment?," *IEEE Wireless Communications Letters*, vol. 10, no. 11, pp. 2547-2551, 2021.

[10] G. Lebrun, J. Gao and M. Faulkner, "MIMO Transmission over a Time-varying Channel Using SVD," *IEEE Transactions on Wireless Communications*, vol. 4, no. 2, pp. 757-764, 2005.

[11] T. J. Willink, "Efficient Adaptive SVD Algorithm for MIMO Applications," *IEEE Transactions on Signal Processing*, vol. 56, no. 2, pp. 615-622, 2008.

[12] E. Telatar, "Capacity of Multi-antenna Gaussian Channels," *European Transactions on Telecommunications*, vol. 10, no. 6, pp. 585–595, 1999.

[13] P. D. Tao and L. T. H. An, "Convex Analysis Approach to DC Programming: Theory, Algorithms and Applications," *Acta Mathematica Vietnamica*, vol. 22, no. 1, pp. 289–355, 1997.

[14] L. T. H. An and P. D. Tao, "The DC (Difference of Convex Functions) Programming and DCA Revisited with DC Models of Real World Nonconvex Optimization Problems," *Annals of Operations Research*, vol. 133, no. 1, pp. 23–46, 2005.

[15] M. Hata, "Empirical Formula for Propagation Loss in Land Mobile Radio Services," *IEEE Transactions on Vehicular Technology*, vol. 29, no. 3, pp. 317-325, 1980.

[16] European Union COST Action 231, "Digital mobile radio towards future generation systems: Final Report," 1999, https://portal.3gpp.org/desktopmodules/Specifications/SpecificationDetails.aspx?specificationId=2430.

[17] I. Siomina and D. Yuan, "Analysis of Cell Load Coupling for LTE Network Planning and Optimization," IEEE Transactions on Wireless Communications, vol. 11, no. 6, pp. 2287-2297, 2012.